Simultaneous expression of cardiac and skeletal muscle isoforms of the L-type Ca^{2+} channel in a rat heart muscle cell line

Rafael Mejía-Alvarez, Gordon F. Tomaselli and Eduardo Marban*

Division of Cardiology, Department of Medicine, The Johns Hopkins University School of Medicine, Baltimore, MD 21205, USA

1. We have investigated the identity of the L-type Ca^{2+} channels present in the H9c2 myoblast line derived from embryonic rat ventricle. To this end, we characterized macroscopic and unitary Ba^{2+} currents through Ca^{2+} channels, and looked for specific genetic messages encoding different L-type Ca^{2+} channel isoforms.

2. The macroscopic Ba^{2+} current (recorded in 10 mM $BaCl_2$) revealed two components with different time courses of activation. The fast component ($I_{Ba,fast}$) activates with a time constant of 23 ± 12 ms (at +10 mV), while the slow component activates with a time constant of 125 ± 12 ms (at +10 mV).

3. Single-channel recordings revealed the presence of two independent channels with conductance values of 11 and 25 pS (in 70 mM Ba^{2+}). These values are identical to those reported previously for skeletal muscle and cardiac Ca^{2+} channels, respectively.

4. The mean ensemble current from the 11 pS channel reproduced the time course of the slow component observed at the macroscopic level, while the 25 pS ensemble time course paralleled that of the fast component.

5. Reverse transcriptase polymerase chain reaction (PCR) with α_1-isoform-specific primers revealed the presence of two distinct transcripts in H9c2 cells. The sequences of the PCR products showed a high degree of homology with the corresponding segments of the rabbit cardiac and skeletal muscle L-type Ca^{2+} channel isoforms. Adult rat skeletal and cardiac muscle expressed only one type of transcript.

6. H9c2 cells appear to be unique in that they simultaneously express both skeletal muscle and cardiac isoforms of the L-type Ca^{2+} channel α_1-subunit. Thus, the H9c2 cell line may prove to be useful when studying the regulation of subtype-specific Ca^{2+} channel gene expression.

Differentiated muscle cells express only the single isoform of the L-type Ca^{2+} channel characteristic of the appropriate muscle lineage (skeletal, cardiac or smooth). Unfortunately, not much is known regarding the control of Ca^{2+} channel gene expression during embryogenesis, due at least partly to the lack of a suitable model in which to study lineage-specific Ca^{2+} channel expression. A cell line capable of expressing multiple isoforms of the L-type Ca^{2+} channel would be useful, therefore, for investigating the factors that determine tissue-specific expression. Genetic homogeneity, ease of availability and genetic manipulation would be some of the advantages of such a model. With this objective in mind, we have characterized the myoblast cell line, H9c2, obtained by Kimes & Brandt (1976) from the embryonic rat heart. These cells have been reported to exhibit properties of either skeletal (depolarizing responses to acetylcholine; Kimes & Brandt, 1976) or cardiac muscle (rapidly activating L-type Ca^{2+} currents; Hescheler, Meyer, Plant, Krautwurst, Rosenthal & Schultz, 1991) after several passages, suggesting that they might be capable of evolving into either phenotype. If this is indeed the case, H9c2 cells may be useful surrogates for genuine precommitment muscle progenitor cells.

When H9c2 cells become confluent (between 2 and 3 weeks of culture), they exhibit a Ba^{2+} current (I_{Ba}) with L-type macroscopic properties. Specifically, this current displays attributes similar to the L-type current recorded from cardiac muscle, i.e. fast activation and cAMP-dependent current enhancement (Hescheler *et al.* 1991). This conclusion is partly supported by the results of a recent investigation in which I_{Ba} was studied at the single-channel level (Sipido & Marban, 1991). After 3–4 weeks of confluence (total time in culture of 5–6 weeks), H9c2 cells were observed to express a voltage-dependent, dihydropyridine (DHP)-sensitive

*To whom correspondence should be addressed.

Ca^{2+} channel with a conductance of 25 pS in 70 mM Ba^{2+}. This conductance is identical to that reported previously for cardiac L-type Ca^{2+} channels (Yue & Marban, 1990). In the same study, however, a conductance level of 13 pS, similar to that reported previously for skeletal muscle L-type Ca^{2+} channels (Rosenberg, Hess, Reeves, Smilowitz & Tsien, 1986; Ma & Coronado, 1988; Hamilton, Mejía-Alvarez, Fill, Hawkes, Schilling & Stefani, 1989; Mejía-Alvarez, Fill & Stefani, 1991) was also observed in a number of patches. On the basis of their unitary current recordings, Sipido & Marban (1991) speculated that H9c2 cells might simultaneously express skeletal and cardiac isoforms of the L-type Ca^{2+} channel.

In order to investigate the molecular identity of the Ca^{2+} channels present in H9c2 cells, we have studied both macroscopic and unitary Ba^{2+} currents, and also screened the cells for the specific messenger RNA encoding each channel isoform. Our results strongly suggest that H9c2 cells simultaneously express both cardiac and skeletal muscle isoforms of the L-type Ca^{2+} channel. Thus, H9c2 cells represent a potentially valuable experimental model with which to study the regulation of subtype-specific Ca^{2+} channel gene expression in muscle cells. A preliminary report of these results has been published (Mejía-Alvarez, Sipido & Marban, 1992).

METHODS

Cell culture

H9c2 cells, derived from the embryonic rat ventricle (cell-line code CRL 1446, passage number 12, obtained from the American Type Culture Collection, Rockville, MD, USA), were grown in Dulbecco's modified Eagle's medium (DMEM; Gibco BRL, Gaithersburg, MD, USA), supplemented with fetal calf serum (10% (v/v), FCS; Gibco BRL), glutamine (2 mM), non-essential amino acids (1% (w/v), MEM Non-Essential Amino Acids Solution, Gibco BRL), penicillin (100 units ml^{-1}) and streptomycin (100 μg ml^{-1}), in an atmosphere of 5% CO_2 in air saturated with water. A stock culture of H9c2 cells was grown in a flask and the cells split every week. From this stock culture, cells were plated onto glass coverslips at a density of approximately 2000 cells per millilitre and cultured as monolayers at 37 °C for 4–6 weeks in DMEM supplemented with 1–10% FCS.

Electrophysiological recordings

Macroscopic and single-channel Ba^{2+} currents through Ca^{2+} channels were recorded at room temperature (24 °C) with an Axopatch 1-D amplifier (CV-4 or IHS-1 headstage; Axon Instruments, Foster City, CA, USA) using either the whole-cell or cell-attached variants of the patch-clamp technique (Hamill, Marty, Neher, Sakmann & Sigworth, 1981). Pipettes were fabricated from borosilicate glass (World Precision Instruments, Sarasota, FL, USA) using a programmable puller (Flaming-Brown, model P-87; Sutter Instruments Company, San Francisco, CA, USA). Ag–AgCl electrodes were used to electrically connect the pipette and bath solutions. The junction potentials between the pipette solution and the reference electrode were nulled prior to obtaining the tight seals (~10 GΩ), after which the pipette capacitance was compensated by the injection of approximately 5 pF of capacitive current. After the membrane was punctured for whole-cell recordings, the series resistance (5–10 MΩ) was compensated electronically, as much as possible, without oscillation (60–75%). The whole-cell data were digitized at 5 kHz with a 12-bit A/D converter (model TL-1 DMA Labmaster; Axon Instruments), filtered using a 4-pole Bessel filter at 1 kHz, and stored in a personal computer for subsequent analysis. Unitary currents were sampled at 10 kHz and filtered at 2 kHz. I_{Ba} was elicited by using depolarizing pulses of variable duration (0·6–1·6 s) to different membrane potentials, from a holding potential (V_h) of −90 mV.

Data analysis

Linear capacitive and leakage components were eliminated from the unitary current traces by digital subtraction of exponential functions fitted to blank sweeps. Idealized current traces were obtained using the half-amplitude criterion (Colquhoun & Sigworth, 1983). Patches containing only one or the other type of channel described below were selected for idealization. The idealized sweeps were used to construct ensemble currents, first-latency curves and open-time histograms. Numerical values are expressed as means ± S.E.M. Electrophysiological data were obtained from thirty-six cells distributed among twenty culture dishes, from six different cell stocks.

Solutions

The composition of the bath solution used to record I_{Ba} was (mM): *N*-methyl-D-glucamine chloride (NMG-Cl), 140; $BaCl_2$, 10; Hepes, 10; glucose, 10 (pH 7·4). The intracellular solution contained (mM): NMG-Cl, 140; EGTA, 10; Hepes, 10; glucose, 10; MgATP, 3 (pH 7·4). Symmetrical NMG-Cl was used (in place of the usual NaCl and KCl) in order to suppress both Na^+ and K^+ currents that might have obscured the recording of I_{Ba}. A high concentration of EGTA was included in the intracellular solution in order to avoid cell damage and mechanical artifacts triggered by Ba^{2+} entry. For the recording of unitary currents the cells were kept in a solution containing a high concentration of K^+ to ensure that the membrane potential would be approximately zero. This solution contained (mM): KCl, 20; potassium glutamate, 120; Hepes, 10; $MgCl_2$, 1; glucose, 10 (pH 7·4). The pipette solution contained (mM): $BaCl_2$, 70; Hepes, 10; glucose, 10 (pH 7·4). The use of Ba^{2+} as the charge carrier instead of Ca^{2+} has several advantages: (a) it blocks many K^+ currents; (b) it permeates almost twice as well as Ca^{2+} through L-type Ca^{2+} channels, thereby increasing the signal-to-noise ratio; and (c) Ca^{2+}-dependent inactivation of the current is eliminated.

Application of drugs

Isoprenaline (Sigma Chemical Company, St Louis, MO, USA) was prepared as a 10 mM stock solution in water. Concentrated (10–50 mM) stock solutions of nifedipine (Sigma) and 1,4-dihydro-2,6-dimethyl-3-nitro-4-(2-trifluoromethylphenyl)-pyridine-5-carboxylic acid methyl ester (Bay K 8644; kindly provided by Dr A. Scriabine, Miles Laboratories Inc., New Haven, CT, USA) were prepared by dissolving the drugs in 100% ethanol. The stock solutions were stored in the dark at −20 °C. The concentrations used in the experiments were obtained by diluting the stock solution with the extracellular recording solution (in the case of the dihydropyridines, the final ethanol concentration was less than 0·01%). During the application of the DHPs the microscope and room lights were turned off.

Control and test extracellular solutions were perfused sequentially into the experimental chamber at a rate of 1–2 ml min^{-1}.

RNA isolation

Total RNA was isolated using a modification of a guanidine isothiocyanate (GuSCN)–caesium chloride (CsCl) method described previously (Tomaselli, Feldman, Yellen & Marban, 1990). Four to six weeks after plating, H9c2 cells (2 g) were harvested and homogenized in 10 ml of a solution containing the following: 4 M GuSCN; 11·2 mg ml^{-1} 2-mercaptoethanol; 100 mM tris(hydroxymethyl)aminomethane hydrochloride (Tris-HCl); pH 7·5. The homogenate was centrifuged at 2200 *g* in an HS-4 rotor (Du Pont Sorvall Instruments, Wilmington, DE, USA) for 5 min at 20 °C. The supernatant was carefully removed and laid onto 2 ml of a solution containing 5·7 M CsCl and 4 mM EDTA. The preparation was centrifuged overnight at 234000 *g* in an SW 50.1 rotor (Beckman Instruments Inc., Fullerton, CA, USA) at 23 °C. The RNA pellet was resuspended in diethylpyrocarbonate (DEPC)-treated water, precipitated from ethanol twice, then washed and resuspended in DEPC water at a concentration of 0·5–1 $\mu g\ \mu l^{-1}$. Total RNA was poly(A)$^+$ enriched by elution from an oligo(dT)-cellulose column using the FastTrack mRNA isolation kit (Invitrogen Corporation, San Diego, CA, USA) following the manufacturer's instructions. An identical protocol was used to isolate RNA from either skeletal or cardiac muscle from adult Sprague–Dawley rats.

Reverse transcription, polymerase chain reaction (PCR) and sequencing of PCR products

The general methods employed for polymerase chain reaction (PCR) amplification of mRNA have been described previously (Gingeras, Davis, Whitfield, Chappelle, DiMichele & Kwoh, 1990). Specifically, first-strand cDNA synthesis was carried out using 1 μg of poly(A)$^+$ RNA, oligo-$(dT)_{12-18}$ primers (500 $\mu g\ ml^{-1}$) and Moloney murine leukaemia virus reverse transcriptase (MMLV-RT; 200 U; Gibco BRL) in the presence of 4 μl of MMLV-RT buffer (5 times concentrated), 2·5 mM deoxynucleotide triphosphates (dNTPs) and 0·1 mg ml^{-1} bovine serum albumin (BSA) in a total volume of 20 μl for 1 h at 37 °C. The reverse transcriptase was heat inactivated by incubation at 95 °C for 3 min. The PCR was performed using Vent-DNA polymerase (1–2 U; New England Biolabs (NEB), Beverly, MA, USA) and either 1 μl of the H9c2 first-strand cDNA synthesis reaction or 100 pmol of rabbit skeletal or heart muscle Ca^{2+} channel α_1-subunit cDNA as template. Paired primers specific for the cardiac or skeletal muscle isoforms were added to give a final concentration of 1 μM each in the presence of Vent-reaction buffer (NEB), dNTPs (300 μM of each), and 100 $\mu g\ ml^{-1}$ BSA in a final reaction volume of 50 μl. The melting temperature was 94 °C; annealing was performed at 56–60 °C for 1 min and extension at 72 °C for 20 s for a total of thirty cycles. The annealing temperatures used varied depending on the template for PCR but were held constant for paired amplifications. Controls used included reactions performed in the absence of reverse transcriptase, cDNA template or oligonucleotide primers. The PCR mixture was run on a 3% agarose gel and the appropriate PCR products isolated using glassmilk (MERmaid, BIO101, La Jolla, CA, USA), according to the manufacturer's instructions. The purified PCR products were sequenced using the double-stranded DNA cycle sequencing system (Gibco BRL). The PCR primers (forward-isoform-specific and reverse-common primers) were end-labelled with ^{32}P and used in the sequencing reactions. The PCR performed using the cardiac–common (*a–c*) primer combination (see Results) generally yielded two distinct products of 400 and 264 bp. The latter band was excised and amplified further to yield the results shown in Figs 8 and 9.

RESULTS

Two types of I_{Ba}

Figure 1 illustrates various time courses of I_{Ba} that were observed in H9c2 cells in culture after 2 weeks of confluence. I_{Ba} was recorded using the whole-cell configuration of the patch-clamp technique, with 10 mM Ba^{2+} as the charge carrier. Figure 1*A* and *B* shows two extreme cases that differ dramatically in their rates of activation. The current in *A* was recorded from a cell that displayed a rapidly activating inward current ($I_{Ba,fast}$), which resembles the activation time course of the L-type Ca^{2+} current (I_{Ca}) recorded in mammalian cardiac myocytes (Isenberg & Klöckner, 1982; Hess & Tsien, 1984). In contrast, other cells predominantly showed a slowly activating inward current ($I_{Ba,slow}$; Fig. 1*B*) with a time course similar to that of I_{Ca} observed in neonatal rat skeletal muscle cells (Donaldson & Beam, 1983; Beam & Knudson, 1988). Extremes such as these were observed in a minority of the cells (6 out of 15); most ($n = 9$) displayed an inward current that clearly reflected a combination of the two types of I_{Ba}. A representative current record from one such 'typical' cell is shown in Fig. 1*C*.

To quantify the differences in the two types of I_{Ba} observed, we measured the activation rates at different membrane potentials in a number of cells (Fig. 2). The raw data (Fig. 2*A*) and monoexponential fits to the data from twelve cells (Fig. 2*B*) reveal that $I_{Ba,fast}$ was activated progressively more rapidly over the range of −10 to +10 mV. In contrast, $I_{Ba,slow}$ was activated much more slowly (Fig. 2*C*), although the rate of activation increased with larger depolarizations (Fig. 2*D*). The difference in the activation rates is illustrated graphically in Fig. 2*D*. A double-exponential function was fitted to a current trace from a typical cell, recorded at +10 mV, showing a combination of the two types of I_{Ba} (Fig. 2*E*). The data points were well fitted when the value of the time constants matched those expected at +10 mV, as indicated in Fig. 2*D* (time constant of activation τ_{fast} was 11 ms and τ_{slow} was 102 ms).

Pharmacological profile of I_{Ba}

We observed that both types of I_{Ba} were sensitive to organic Ca^{2+} channel modulators such as the DHPs, Bay K 8644 and nifedipine. Figure 3*A* shows that Bay K 8644 (2 μM) increased the current amplitude at 0 mV, and decreased the rate of the tail-current decay. The potentiating effect of Bay K 8644 on the current was particularly prominent at negative potentials (Fig. 3*B*); there was a 15 mV shift of

the activation curve towards more negative potentials. Similar results were also seen in two other cells. Both components of I_{Ba} also appeared to be sensitive to β-adrenergic stimulation (Fig. 3*C* and *D*); addition of 10 μM isoprenaline increased the current at most potentials, although once again the current–voltage (I–V) relation exhibited a negative shift of the activation curve (Fig. 3*D*). Similar effects were also observed in two other cells. The addition of 100 μM $CdCl_2$ (Fig. 3*D*) or 10 μM nifedipine (two cells, data not shown) blocked I_{Ba}. The pharmacological properties of $I_{Ba,slow}$ and $I_{Ba,fast}$ indicate that the channels responsible for these currents are probably L-type Ca^{2+} channels (Bean, 1989). In order to confirm the identity of these channels, we measured I_{Ba} at the single-channel level.

Two different unitary conductances

Figure 4*A* shows selected traces illustrating the single-channel activity at various membrane potentials. The unitary currents were recorded from a cell-attached patch in H9c2 cells with 70 mM $BaCl_2$ as the charge carrier. The currents were elicited by depolarizing the membrane for 650 ms to the potentials indicated, from a holding potential of −90 mV. Two unitary current amplitudes (indicated by the dashed lines in Fig. 4*A*) were clearly resolvable, as was also confirmed by the amplitude histograms (Fig. 4*A*, right column). Opening events representative of both amplitudes coexist in the traces at +5 and +10 mV. The corresponding I–V relations (Fig. 4*B*) reveal unitary conductance values of 11 pS ($n = 6$) and 25 pS ($n = 8$), respectively. We concluded that these conductances arose from two independent channels, a conclusion based on the following observations: (a) interconverting opening events were never observed, although superimposed openings were common (e.g. at +10 mV in Fig. 4*A*); and (b) only one or the other conductance was observed in four patches (although the presence of both conductances in the same patch was the most common observation; $n = 10$).

The identity of these channels was investigated individually by examining their DHP sensitivity and gating kinetics. A summary of the results of these experiments is shown in Figs 5 and 6. These show selected traces both before and after the addition of 2 μM Bay K 8644 (*A* and *B*, respectively, in both figures). Figure 5 shows the results from a patch containing a single low-conductance channel. Prior to the addition of the drug, the single-channel activity consisted of brief sporadic opening events, with numerous blank sweeps (65%). After the addition of the Ca^{2+} channel agonist, the open probability (P_o) was enhanced dramatically; the openings were longer (indicative of mode-2 gating kinetics; Hess, Lansman & Tsien, 1984; Rosenberg *et al.* 1986) and more frequent, and the number of blank sweeps was also significantly lower (32%). Subconductance levels were not

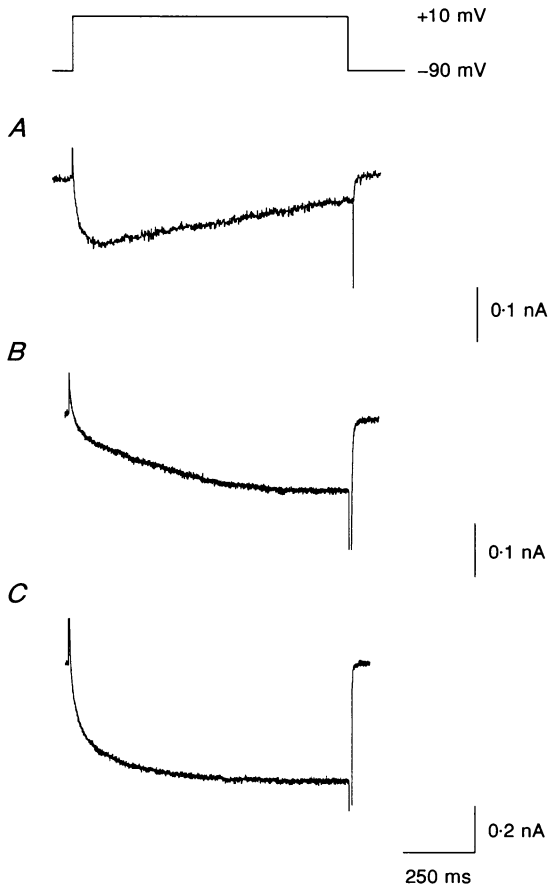

Figure 1. Illustration of three different time courses of I_{Ba}
Inward currents were recorded in the whole-cell configuration, in the presence of 10 mM $BaCl_2$, by depolarizing the membrane to +10 mV for 975 ms, from a holding potential of −90 mV (the pulse protocol is shown at the top of the figure). I_{Ba} can exhibit three different morphologies. To illustrate this variability, traces from three different cells are shown. *A* illustrates a fast-activating current ($I_{Ba,fast}$) similar to that described for cardiac muscle, predominant in a small number of cells; *B* illustrates a skeletal muscle-like current ($I_{Ba,slow}$), characterized by a slow activation, displayed by other cells; and *C* illustrates a combination of the two components, exhibited by the majority of the cells.

detected either under control conditions or after the addition of the drug. The open-time histogram shown in Fig. 5*C* was constructed from 110 traces recorded in the presence of Bay K 8644. The frequency distribution was well described by the sum of two exponentials:

$$y = (W_1/\tau_1)(e^{-t/\tau_1}) + (W_2/\tau_2)(e^{-t/\tau_2}), \quad (1)$$

where W_1 and W_2 are the total numbers of events characterized by the time constants τ_1 and τ_2. The slow component represents the long-lasting events with a mean open time of about 12 ms. A conductance value of 11·6 pS was determined from a ramp pulse (Fig. 5*D*).

The DHP sensitivity and kinetics of the 25 pS channel were investigated using the same experimental protocol as that for the 11 pS channel. Figure 6*A* shows selected traces of the channel activity recorded under control conditions, characterized by a low P_o (75% blank sweeps from a total of 300 sweeps). After the addition of 2 μM Bay K 8644 the activity increased significantly (Fig. 6*B*). Blank sweeps were less frequent (49% from a total of 250 sweeps) and individual openings lasted for a longer period and were more frequent (mode-2 gating). The open-time histogram (Fig. 6*C*), constructed from 250 traces recorded in the presence of 2 μM Bay K 8644, was well fitted by two

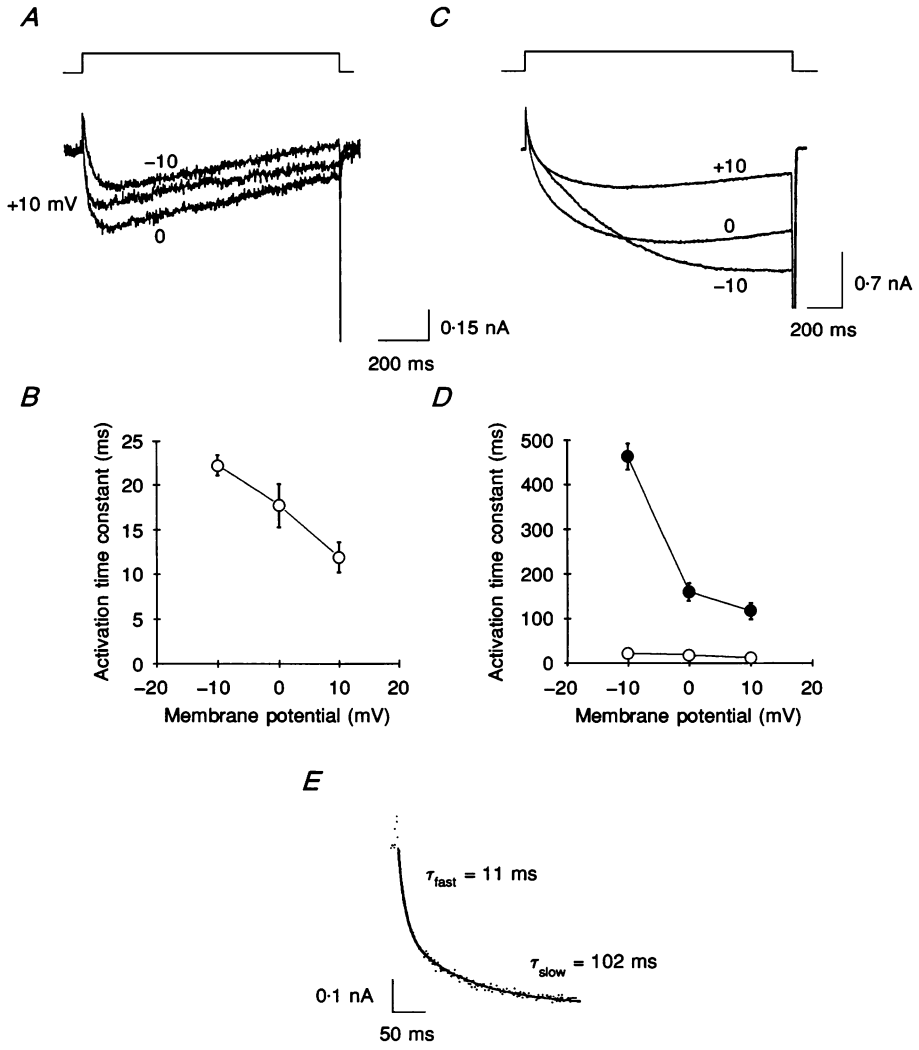

Figure 2. Voltage dependence of the activation rates

A, I_{Ba} recorded under the same experimental conditions as in Fig. 1. $I_{Ba,fast}$ was elicited by depolarizing pulses of 1 s to the membrane potentials indicated, from a V_h of −90 mV. The activation phase is more rapid at more positive potentials. *B*, a monoexponential function was fitted to the activation phase of $I_{Ba,fast}$, and the resulting time constant plotted as a function of the membrane potential. Data were collected from 12 cells. *C*, $I_{Ba,slow}$ recorded in the presence of 2 μM Bay K 8644 using 1·5 s depolarizing pulses to the same membrane potentials as in *A*. *D*, time constant of the exponential functions fitted to the activation phase of $I_{Ba,slow}$ (●) plotted as a function of the membrane potential. Data were collected from 12 cells. For comparison, the activation rates from $I_{Ba,fast}$ are also shown (○). *E*, a double-exponential curve was fitted to I_{Ba} recorded at +10 mV from a cell showing both the fast and slow components.

exponential distributions (eqn (1)). The unitary conductance was 26 pS (Fig. 6*D*).

From our observations concerning DHP sensitivity and gating properties, we can confidently conclude that the two channels are L-type Ca^{2+} channels. In fact, the unitary conductance values of 25 and 11 pS are practically identical to those reported previously for cardiac (Rosenberg *et al.* 1986; Yue & Marban, 1990) and skeletal muscle (Ma & Coronado, 1988; Mejía-Alvarez *et al.* 1991) L-type Ca^{2+} channels, respectively. These observations support our original hypothesis that H9c2 cells simultaneously express cardiac and skeletal muscle isoforms of the Ca^{2+} channel and that the two channel types underlie the two- component I_{Ba} observed at the whole-cell level. In order to test these conclusions further, we reconstructed the macroscopic properties of the currents that would be predicted from the single-channel data.

Activation rates at the single-channel level

To determine the probable influence of each of the unitary currents on the macroscopic currents, we obtained mean ensemble currents from 500 sweeps, collected by depolarizing the membrane to +10 mV. The resulting mean ensemble currents are shown in Fig. 7. The ensemble current shown in Fig. 7*A* was generated from the 25 pS single-channel activity, scaled and superimposed on the macroscopic current recorded from a cell expressing predominantly $I_{Ba,fast}$. The single-channel and whole-cell records were both obtained in the presence of Bay K 8644. The macroscopic currents were offset by a factor of 10 mV to compensate for the surface charge effect introduced by the different Ba^{2+} concentrations used in the single-channel and whole-cell experiments (McLaughlin, Szabo & Eisenman, 1971). The activation phase of the cardiac-type ensemble current and $I_{Ba,fast}$ are shown with an expanded time base (Fig. 7*A*). The similarity of the time course of both currents is further emphasized by the values of the activation time constants obtained. In an analogous manner, $I_{Ba,slow}$ is well matched by the ensemble current trace generated from an 11 pS channel (Fig. 7*B*).

Specific genetic message for each isoform

In order to obtain complementary evidence of the simultaneous expression of cardiac and skeletal muscle isoforms of the Ca^{2+} channel in H9c2 cells, we looked for the specific genetic messages for each isoform. The

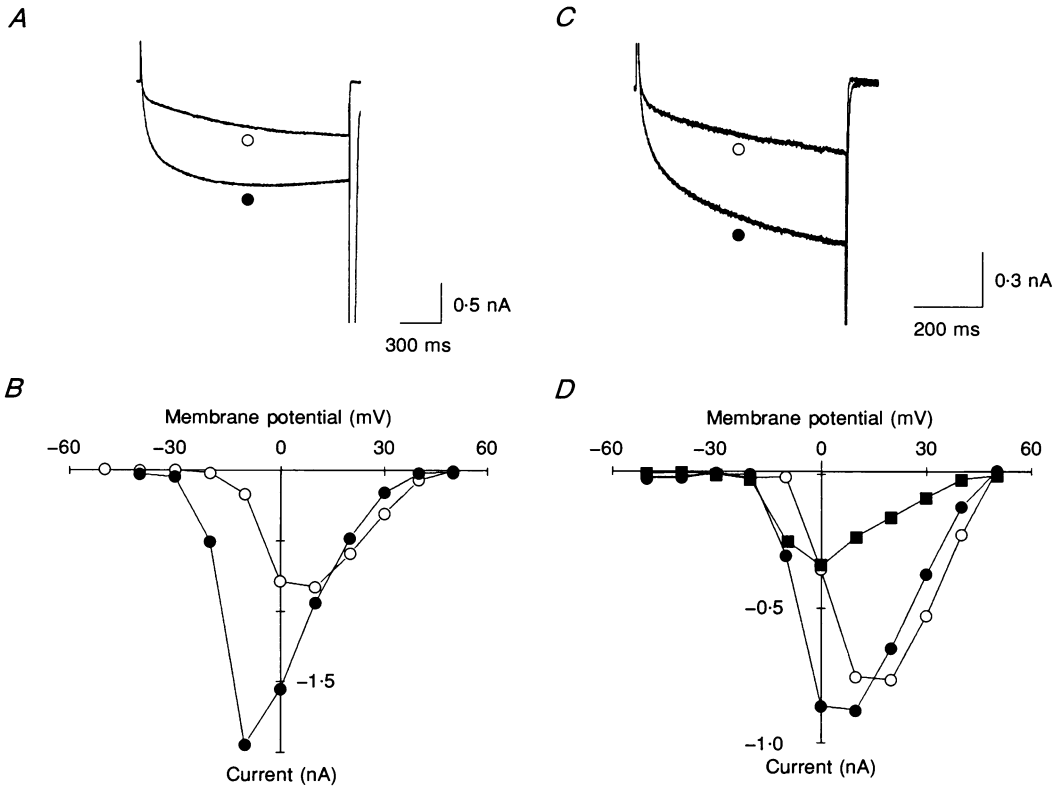

Figure 3. Pharmacological profile of I_{Ba}
A, I_{Ba} was recorded with 10 mM Ba^{2+} before (○) and after (●) the addition of 2 μM Bay K 8644, using 1·5 s depolarizing pulses to 0 mV, from a V_h of −90 mV. Tail currents were recorded at −90 mV. *B*, peak current–voltage relations from the same cell recorded under control conditions (○) and after the addition of Bay K 8644 (●). *C*, I_{Ba} recorded at 0 mV, from a V_h of −90 mV, before (○) and after (●) the addition of 10 μM isoprenaline. *D*, current–voltage relations from the same cell under control conditions (○), after isoprenaline (●) and after partially blocking the current with 100 μM $CdCl_2$ (■).

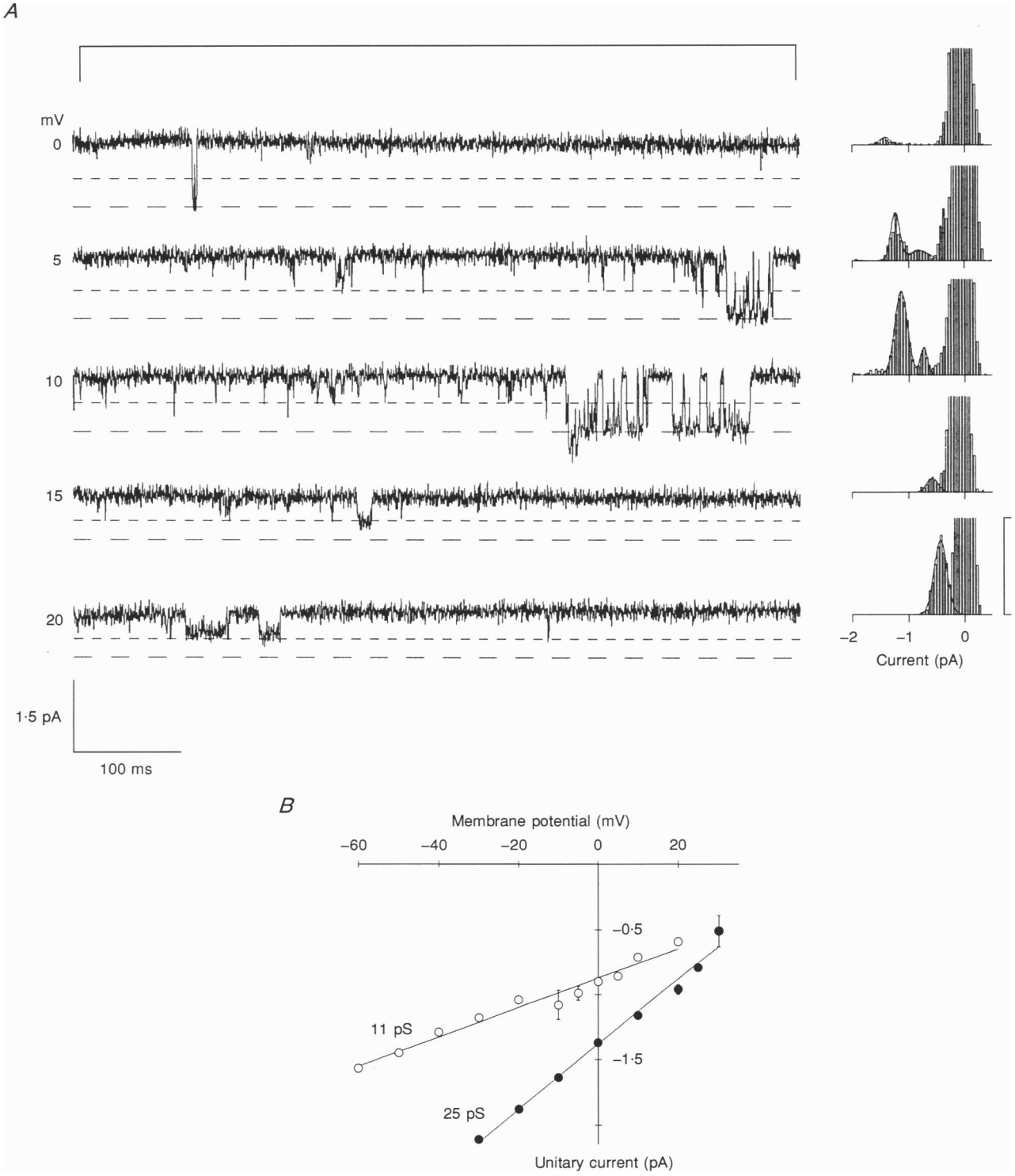

Figure 4. Illustration of two different unitary conductances
A, single-channel activity was recorded using the cell-attached configuration, with 70 mM $BaCl_2$ in the pipette solution and 140 mM K^+ in the bath solution. Unitary currents were elicited by depolarizing the membrane for 650 ms to different potentials (indicated at the left of the traces) from a V_h of −90 mV. Opening events are shown as downward deflections. Two different current amplitudes (indicated by dashed lines) were identified in the corresponding amplitude histograms (shown at the right of each sweep; vertical bar = 100 events). *B*, unitary current amplitudes plotted as a function of the membrane potential. Data points represent mean values from 6 cells (11 pS) and 8 cells (25 pS) and were fitted (lines) by least squares. Error bars are shown when the S.E.M. exceeded the symbol size.

polymerase chain reaction was used to amplify isoform-specific regions of the L-type Ca^{2+} channel mRNA. The PCR experiments were designed to amplify the part of the segment linking repeats I and II. This putative cytoplasmic loop was selected because there is little homology in this region between the cardiac and the skeletal muscle isoforms of the α_1-subunit from the rabbit (Tanabe *et al.* 1987; Mikami *et al.* 1989). Two forward primers, corresponding to isoform-specific regions (arrows *a* and *b*, Fig. 8*A*), and one reverse primer complementary to a highly conserved region (the first membrane-spanning segment of the second homologous repeat (II-S1)) shared by both isoforms (arrow *c*) were used. The primers selected showed little homology to other regions of the Ca^{2+} channel or to other known voltage-dependent ion channels.

Poly $(A)^+$-selected RNA was isolated from H9c2 cells and reverse transcribed to produce the corresponding cDNA, which was then used as the template for the PCR. The combination of either forward primer with the reverse primer consistently produced one of two specific PCR products, distinguishable by their molecular weights (Fig. 8*B*). When the cardiac primer (*a*) was used in combination with the common primer (*c*), a segment of 264 bp was generated (lane H9c2 *a–c*, Fig. 8*B*). In contrast, when the skeletal muscle primer (*b*) was used a 200 bp segment was amplified (lane H9c2 *b–c*, Fig. 8*B*). When the cDNA encoding the α_1-subunit of the Ca^{2+} channel from rabbit heart or skeletal muscle was used as the template with the corresponding isoform-specific primer pair, the expected 264 and 200 bp fragments were generated (heart *a–c* and skeletal muscle *b–c*, Fig. 8*B*). Reactions of the *b–c* primer combination with cardiac muscle cDNA produced no amplified bands, nor did the converse pairing (*a–c* with skeletal muscle cDNA; data not shown). A comparison of the expression patterns derived from adult rat muscle (skeletal or cardiac) tissues with those in H9c2 cells is shown in Fig. 8*C*. The *b–c* primer recognized a band of the appropriate size in the skeletal muscle tissue RNA, but not in the cardiac tissue RNA. Conversely, the *a–c* primers amplified a band of the appropriate size from cardiac-derived RNA, but no amplification occurred in the sample from skeletal muscle. As shown previously, H9c2-derived

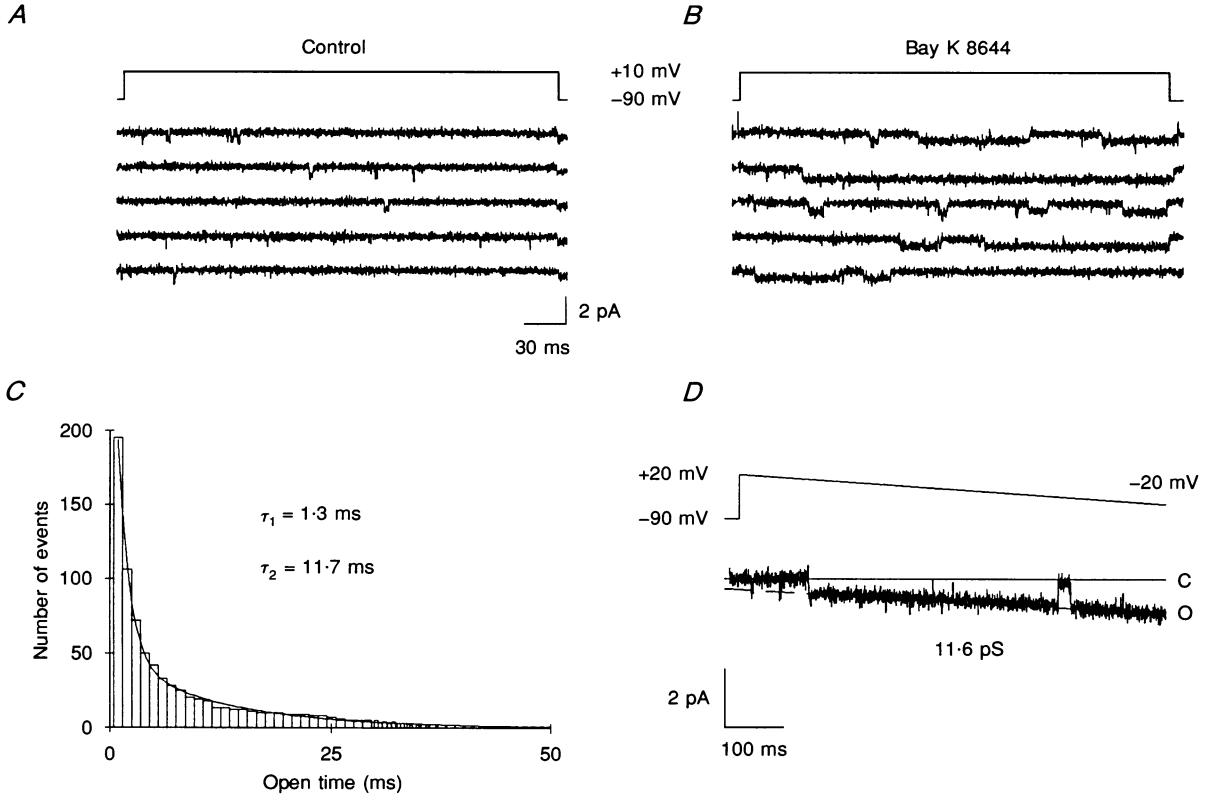

Figure 5. DHP sensitivity and gating kinetics of the 11 pS channel
A, control activity recorded by depolarizing the membrane to +10 mV for 300 ms from a V_h of −90 mV. *B*, single-channel activity recorded with the same pulse protocol after the addition of 2 μM Bay K 8644. *C*, open-time histogram constructed from 110 traces recorded in the presence of Bay K 8644 using the same pulse protocol. The bin width of the histogram is 1 ms. A double-exponential curve (eqn (1)) was fitted to the frequency distribution using a non-linear least squares method. The time constant of each exponential component is indicated. *D*, unitary conductance measured using a 750 ms depolarizing pulse from +20 to −20 mV from a V_h of −90 mV. Dashed line (O) indicates the least squares fit to the amplitude of the current. The closed level is indicated by the continuous line (C).

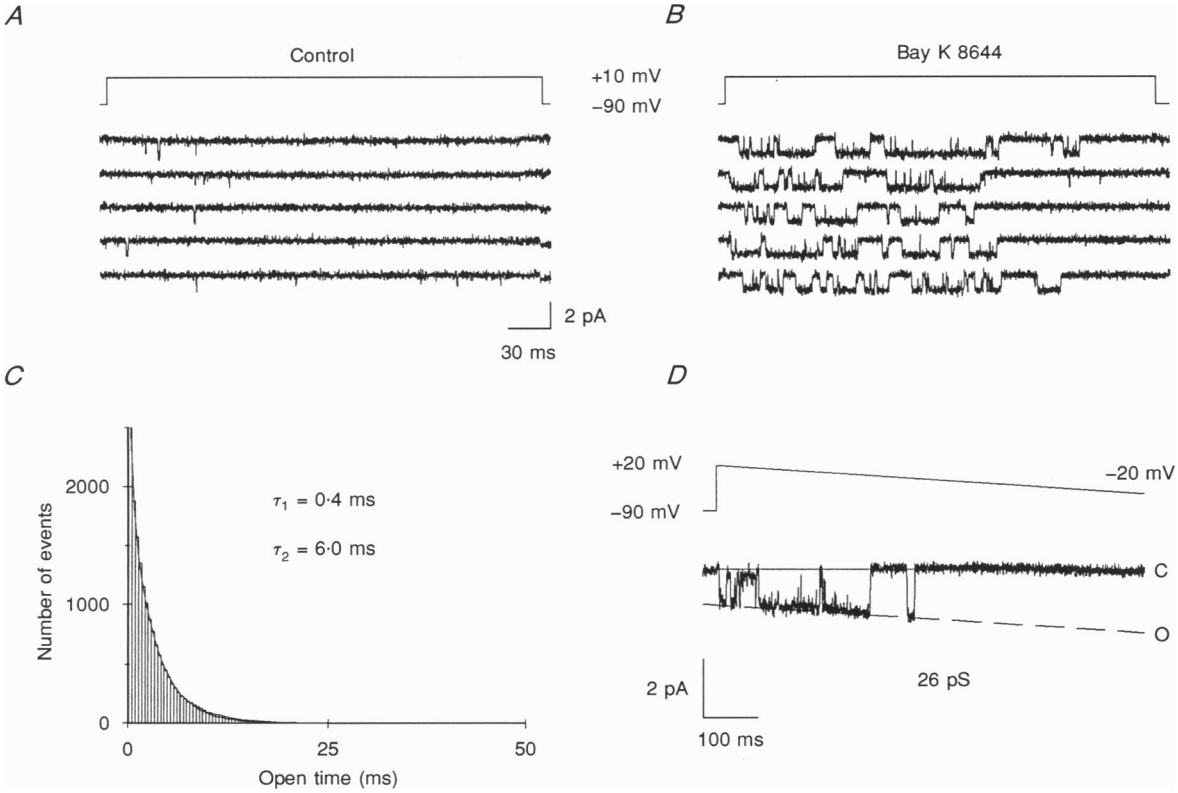

Figure 6. DHP sensitivity and gating kinetics of the 25 pS channel
A and *B*, single-channel activity recorded with the same pulse protocol used in Fig. 5 before and after the addition of 2 μM Bay K 8644. *C*, open-time histogram constructed from 250 traces recorded in the presence of Bay K 8644 using the same pulse protocol. The bin width of the histogram is 400 μs. A double-exponential curve (eqn (1)) was fitted to the frequency distribution using the same method as that for the 11 pS channel. *D*, unitary conductance measured using the same pulse protocol as for the 11 pS channel (Fig. 5*D*).

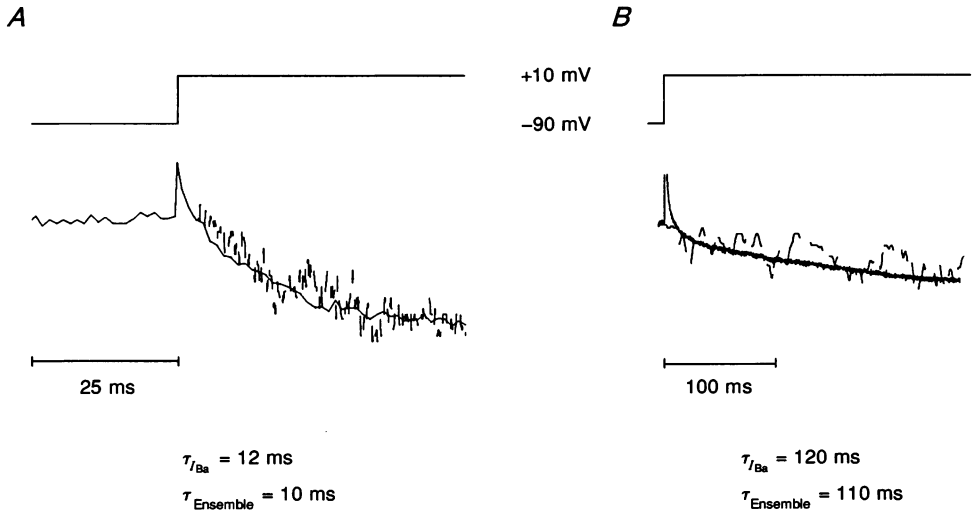

Figure 7. Comparison of the activation rates of I_{Ba} and ensemble currents
A, ensemble current obtained from a 25 pS channel (interrupted line) scaled and superimposed on $I_{Ba,fast}$. *B*, ensemble current (interrupted line) constructed from an 11 pS channel scaled and superimposed on $I_{Ba,slow}$. The time constant values of the exponential functions fitted to each current are indicated below the traces; continuous line $\tau_{I_{Ba}}$; interrupted line $\tau_{Ensemble}$.

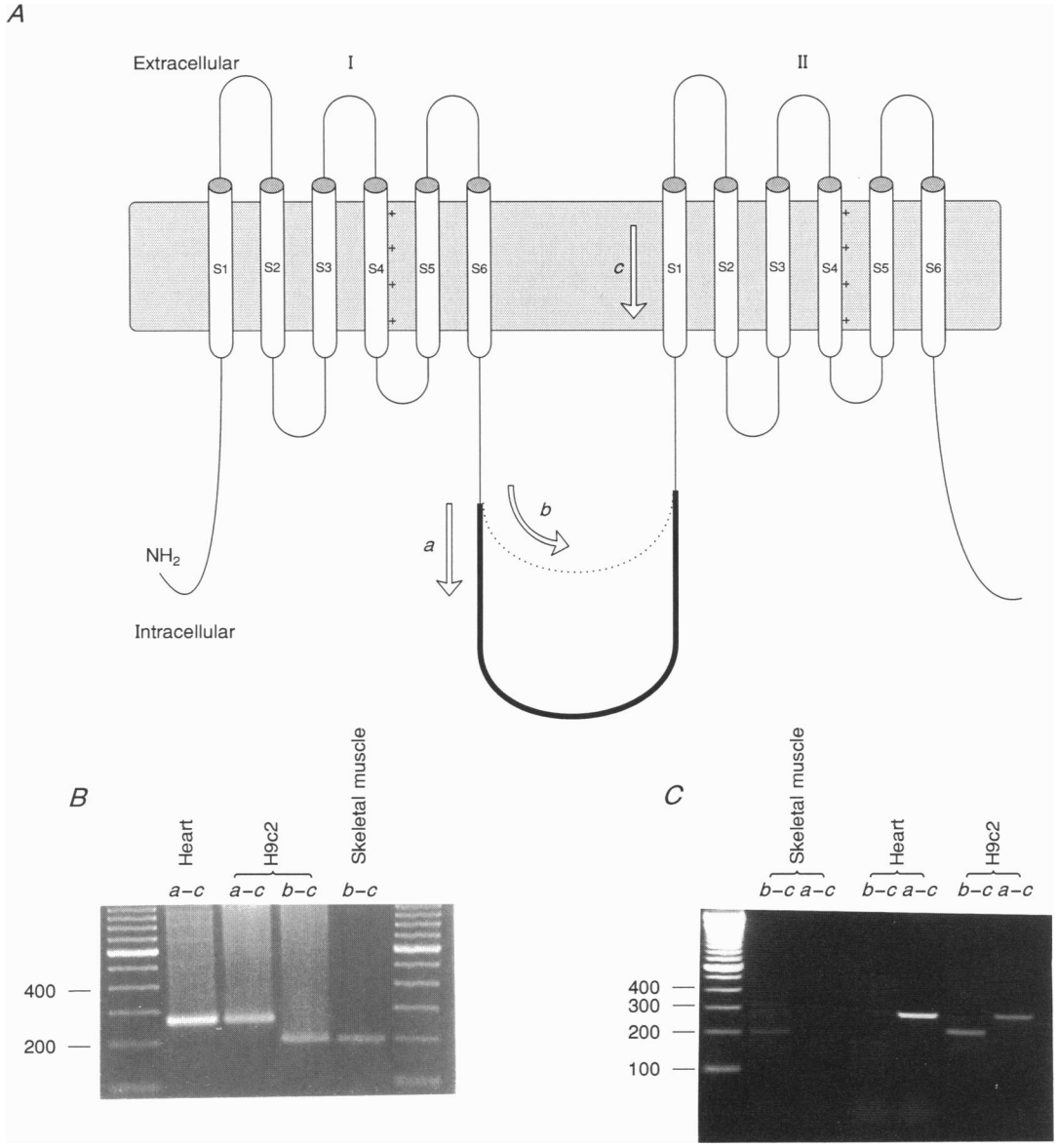

Figure 8. Primer design and PCR products from the rat-derived H9c2 cell line and adult rat tissues

A, cDNA from the I–II loop of the α_1-subunit of the Ca^{2+} channel gene from H9c2 cells was amplified using standard PCR techniques. Two forward primers (5′ end) were designed to anneal to unique regions of the I–II loop from either the cardiac muscle (arrow *a*; residues 1419–1440 of the reported sequence; continuous bold line) or the skeletal muscle (arrow *b*; residues 1116–1137; dotted line) isoforms of the gene based on the sequences from the rabbit. A reverse primer (3′ end) was designed to hybridize with a highly conserved region of the II-S1 from both isoforms of the gene (arrow *c*; residues 1663–1682 for cardiac and 1297–1317 for skeletal). *B* and *C* show PCR products separated by agarose gel electrophoresis. *B*, the left and right lanes contain molecular weight markers (in steps of 100 bp). Lane labelled Heart *a–c* contains the PCR product of the rabbit cardiac Ca^{2+} channel α_1-subunit cDNA amplified with primers *a* and *c*, which border a known region of 264 bp. Lanes labelled H9c2 *a–c* and *b–c* represent PCR products from the rat-derived H9c2 Ca^{2+} channel gene using either primers *a* and *c* or primers *b* and *c*. Lane labelled Skeletal muscle *b–c* contains the PCR product of the rabbit skeletal muscle Ca^{2+} channel α_1-subunit cDNA amplified using primers *b* and *c*, which define a region of 200 bp. *C*, the same PCR primers were used to amplify identical products from adult rat heart (Heart) and skeletal muscle. Using cardiac primers (*a–c*), a 264 bp fragment was isolated from rat heart cDNA, while the skeletal muscle primer pair (*b–c*) generated no products. The converse experiment in rat skeletal muscle produced a 200 bp fragment when the skeletal muscle primer pair was used, but no products with the cardiac primer pair. Amplification from H9c2 cells produced the appropriate PCR products using either primer pair. The left lane contains molecular weight markers as in *B*.

RNA clearly exhibited both transcripts. Negative controls excluding either the template DNA or primers from the reaction mixture or the use of an unrecognized template produced no PCR products. Similarly, no PCR products were generated when the reverse-transcriptase step was omitted, a result that argues against the possibility of genomic leak. The results were confirmed in ten separate rounds of PCR amplification.

In order to establish the identity of the H9c2 Ca^{2+} channel gene segments, the two PCR products obtained were sequenced and a comparison made with the corresponding sequences reported previously for the rabbit isoforms of the Ca^{2+} channel. Figure 9 shows the alignment of the cDNA and the derived amino acid sequences from the H9c2 Ca^{2+} channel gene isoforms (presumably of rat origin) with the comparable sequences from rabbit heart and skeletal muscle (Tanabe *et al.* 1987; Mikami *et al.* 1989). The cardiac isoform exhibited 91% homology at the nucleotide level and 98% homology at the amino acid level, while the skeletal muscle isoform showed 88 and 87% homology at the nucleotide and the amino acid levels, respectively. The striking similarities with the published sequences from the rabbit, particularly at the deduced protein level, indicate that it is probable that these PCR products do in fact arise from distinct mRNAs encoding the two isoforms of the α_1-subunit of the L-type channel.

DISCUSSION

Time course of $I_{Ba,slow}$ and $I_{Ba,fast}$

Our results show that H9c2 cells simultaneously express two different isoforms of the L-type Ca^{2+} channel. The Ba^{2+} currents that these channels mediate are distinguishable at the macroscopic level by their different activation time courses. One of the currents, $I_{Ba,slow}$, exhibits activation gating similar to that observed in I_{Ca} recorded in adult skeletal muscle from the frog (time constant of activation (τ_a) 100 ms at +10 mV, in 10 mM Ca^{2+}, at room temperature; Sánchez & Stefani, 1983) and from the rat (time-to-peak 150 ms, at +10 mV, in 10 mM Ca^{2+}, at room temperature; Donaldson & Beam, 1983; τ_a 55 ms, at 0 mV, in 2 mM Ca^{2+}, at room temperature; Mejía-Alvarez *et al.* 1991). In contrast, $I_{Ba,fast}$ exhibits activation kinetics an order of magnitude faster, with a time course comparable to that recorded from bovine (τ_a 0·5 ms, at +10 mV, 35 °C; Isenberg & Klöckner, 1982) and guinea-pig (time-to-peak 3 ms, at 0 mV, in 3·6 mM Ca^{2+}, at 36 °C; Trautwein & Pelzer, 1985) ventricular myocytes. Although a direct comparison of our results with those reported previously is made complicated by differences in the experimental conditions used, the activation rates of $I_{Ba,slow}$ and $I_{Ba,fast}$ that we observed are certainly consistent with the time courses of I_{Ca} and I_{Ba} reported previously in skeletal and cardiac muscle, respectively.

The similarities in the activation rates, voltage dependence and sensitivity to the effects of DHPs and Cd^{2+} provide support for the hypothesis that $I_{Ba,slow}$ in H9c2 cells and the slow I_{Ca} in skeletal muscle represent identical or closely related channel proteins. Similarly, we also conclude that $I_{Ba,fast}$ might reflect the expression of a cardiac isoform of the L-type Ca^{2+} channel.

Comparison with other Ca^{2+} currents

The cardiac T-type Ca^{2+} current ($I_{Ca,T}$) is similar to $I_{Ba,fast}$ in several ways. $I_{Ca,T}$ exhibits a rapid activation rate and inactivates in a purely voltage-dependent manner. However, unlike $I_{Ba,fast}$, $I_{Ca,T}$ activates at more negative potentials (−50 mV with 5 mM Ba^{2+}; Hirano, Fozzard & January, 1989) and is not sensitive to DHPs.

From the purely electrophysiological point of view it is difficult to rule out the possibility that a non-cardiac L-type Ca^{2+} channel might be responsible for $I_{Ba,fast}$. The neuronal L-type I_{Ca} could be one such candidate. This is similar to $I_{Ba,fast}$ in the following ways: (a) it activates in the same voltage range; (b) it displays a similar time course; (c) it has an identical single-channel conductance (25 pS, in 110 mM Ba^{2+}; Fox, Nowycky & Tsien, 1987); (d) it is sensitive to Cd^{2+} block; and (e) it may be modulated by β-adrenergic stimulation (Gray & Johnston, 1987). However, unlike $I_{Ba,fast}$, the neuronal L-type Ca^{2+} channels are essentially unaffected by the dihydropyridine blocker nifedipine at a V_h of −80 mV (Fox *et al.* 1987; Bean, 1989). In addition, the molecular sequence data are distinct from the comparable segment of the neuronal L-type channel (Williams *et al.* 1992).

An L-type Ca^{2+} current that exhibits similar activation kinetics and comparable pharmacological properties to $I_{Ba,fast}$ has been recorded in dysgenic skeletal muscle ($I_{Ca,dys}$; Adams & Beam, 1989). However, $I_{Ca,dys}$ displays little or no decay during depolarizing pulses lasting up to 200 ms, even when recorded in 10 mM Ca^{2+}. In contrast, $I_{Ba,fast}$ shows a significant voltage-dependent decay (Fig. 1*A*) that is comparable to the inactivation observed in cardiac I_{Ca} (Lee & Tsien, 1984). These results suggest that the channel mediating $I_{Ca,dys}$ is distinct from that responsible for $I_{Ba,fast}$ in H9c2 cells.

The dihydropyridine-sensitive Ca^{2+} current of frog skeletal muscle has been observed to be capable of fast-activation gating after conditioning depolarization (Garcia, Avila-Sakar & Stefani, 1990; Feldmeyer, Melzer, Pohl & Zöllner, 1992). However, this fast type of gating would not be expected to figure prominently under our experimental conditions.

Unitary currents

A more sensitive approach to distinguish between two related isoforms of ion channel proteins is the measurement of single-channel conductance and gating kinetics. Using this approach, we observed that H9c2 cells exhibit two different unitary conductance levels (of 11 and 25 pS), which probably arise from two different and independent Ca^{2+} channels. This hypothesis is supported by the

H9c2 264 bp fragment: rabbit cardiac muscle α_1-subunit

```
H9c2     GCA GAA GAC ATC GAC CCT GAG AAT GAG GAC GAG GGC ATG GAT GAA GAC AAA CCC CGA AAC
           Ala Glu Asp Ile Asp Pro Glu Asn Glu Asp Glu Gly Met Asp Glu Asp Lys Pro Arg Asn
           Ala Glu Asp Ile Asp Pro Glu Asn Glu Asp Glu Gly Met Asp Glu Glu Lys Pro Arg Asn
Cardiac  GCA GAA GAC ATC GAC CCT GAG AAT GAG GAT GAA GGC ATG GAT GAG GAG AAA CCC CGA AAC

H9c2     ATG AGC ATG CCT ACA AGT GAG ACT GAG TCT GTC AAC ACC GAA AAC GTG GCT GGA GGT GAC
           Met Ser Met Pro Thr Ser Glu Thr Glu Ser Val Asn Thr Glu Asn Val Ala Gly Gly Asp
           Met Ser Met Pro Thr Ser Glu Thr Glu Ser Val Asn Thr Glu Asn Val Ala Gly Gly Asp
Cardiac  ATG AGC ATG CCT ACA AGT GAG ACC GAA TCT GTC AAC ACT GAA AAC GTG GCT GGA GGT GAC

H9c2     ATC GAG GGT GAA AAC TGT GGA GCC CGG CTT GCC CAC CGG ATC TCC AAA TCC AAG TTC AGC
           Ile Glu Gly Glu Asn Cys Gly Ala Arg Leu Ala His Arg Ile Ser Lys Ser Lys Phe Ser
           Ile Glu Gly Glu Asn Cys Gly Ala Arg Leu Ala His Arg Ile Ser Lys Ser Lys Phe Ser
Cardiac  ATC GAA GGA GAA AAC TGC GGG GCC AGG CTG GCC CAC CGG ATC TCC AAG TCG AAA TTC AGC

H9c2     CGC TAC TGG CGC CGG TGG AAT AGA TTC TGC AGA AGA AAG TGC CGT GCC GCA GTT AAG TCC
           Arg Tyr Trp Arg Arg Trp Asn Arg Phe Cys Arg Arg Lys Cys Arg Ala Ala Val Lys Ser
           Arg Tyr Trp Arg Arg Trp Asn Arg Phe Cys Arg Arg Lys Cys Arg Gly Ala Val Lys Ser
Cardiac  CGC TAC TGG CGC CGG TGG AAT AGG TTC TGC AGG AGA AAG TGC CGC GGA GCG GTC AAG TCG

H9c2     AAC GTC TTC TAC TGG CTG GTG ATG
           Asn Val Phe Tyr Trp Leu Val Met
           Asn Val Phe Tyr Trp Leu Val Met
Cardiac  AAC GTC TTC TAC TGG CTG GTG ATG
```

H9c2 200 bp fragment: rabbit skeletal muscle α_1-subunit

```
H9c2     CGC GAG GTC ATG GAC GTG GAG GAC TTG AGA GAA GGC AAG CTG TCT TTG GAT GAA GGG GGC
           Arg Glu Val Met Asp Val Glu Asp Leu Arg Glu Gly Lys Leu Ser Leu Asp Glu Gly Gly
           Arg Glu Val Met Asp Val Glu Asp Leu Arg Glu Gly Lys Leu Ser Leu Glu Glu Gly Gly
Skeletal GGC GAG GTC ATG GAC GTG GAG GAC CTG AGA GAA GGA AAG CTG TCC TTG GAA GAG GGA GGC

H9c2     TCC GAC ACG GAA AGC CTG TAC GAA ATC GAG GGC TTG AAC AAA ATC ATC CAG TTC ATC CGA
           Ser Asp Thr Glu Ser Leu Tyr Glu Ile Glu Gly Leu Asn Lys Ile Ile Gln Phe Ile Arg
           Ser Asp Thr Glu Ser Leu Tyr Glu Ile Glu Gly Leu Asn Lys Ile Ile Gln Phe Ile Arg
Skeletal TCG GAT ACA GAG AGC TTA TAT GAA ATC GAG GGC TTG AAC AAA ATC ATC CAA TTC ATT CGG

H9c2     CAC TGG CGG CAG TGG AAT CGC GTC TTC CGC TGG AAG TGC CAT GAC CTA GTG AAA TCC AAG
           His Trp Arg Gln Trp Asn Arg Val Phe Arg Trp Lys Cys His Asp Leu Val Lys Ser Lys
           His Trp Arg Gln Trp Asn Arg Val Phe Arg Trp Lys Cys His Asp Leu Val Lys Ser Arg
Skeletal CAC TGG AGG CAG TGG AAC CGT GTC TTC CGC TGG AAG TGC CAT GAC CTG GTG AAG TCC AGA

H9c2     GTC TTC TAC TGG CTG GTC ATC
           Val Phe Tyr Trp Leu Val Ile
           Val Phe Tyr Trp Leu Val Ile
Skeletal GTC TTC TAC TGG CTG GTC ATC
```

Figure 9. Nucleotide and deduced amino acid sequences from the PCR products of the rat-derived H9c2 Ca^{2+} channel α_1-subunit gene

Sequences of the PCR products of the cardiac and skeletal muscle isoforms of the H9c2 Ca^{2+} channel gene aligned with the reported sequence from rabbit heart (Cardiac; Mikami *et al.* 1989) and rabbit skeletal muscle (Skeletal; Tanabe *et al.* 1987). Mismatches at the nucleotide level are indicated by bold letters. Differences in the deduced amino acid sequence (three-letter code) are indicated by italics. The lines below the nucleotide sequences indicate the PCR primer sequences.

following observations: (a) the 11 and the 25 pS channels gate with an independence that is statistically significant (the observation of patches with a single conductance level supports this statement); and (b) transformations of one current amplitude into the other were never observed.

Additional support for the presence of two independent channels can be gleaned from the differences in gating kinetics displayed by the channels in response to the Ca^{2+} channel agonist Bay K 8644. In the absence of the agonist, the open-time histogram is well described by a single exponential probability-density function, with a time constant of less than 1 ms for the cardiac channel (at +10 mV; Hess *et al.* 1984; Lacerda & Brown, 1989). In the presence of Bay K 8644 an additional slower component has been observed, with a time constant of approximately 20 ms for the cardiac channel (+10 mV, 5 μM Bay K 8644; Hess *et al.* 1984; +20 mV, 1 μM Bay K 8644; Lacerda & Brown, 1989), and 30 ms for the skeletal muscle channel (−10 mV, 0·3 μM Bay K 8644; Ma, Mundiña-Weilenmann, Hosey & Ríos, 1991). In our study, we also observed that the open-time histograms from both H9c2 channels recorded in the presence of 2 μM Bay K 8644 are well described by two exponential distributions. Furthermore, the skeletal muscle channel displays longer mean open times (τ_1, 1 ms and τ_2, 12 ms) than the cardiac channel (τ_1, 0·4 ms and τ_2, 6 ms). Our data are in general agreement with the observation that skeletal muscle Ca^{2+} channels in lipid bilayers gate somewhat more slowly than cardiac Ca^{2+} channels. However, kinetic data obtained from lipid bilayer experiments should be interpreted with caution since the lipid composition of the bilayer may affect single-channel gating kinetics (Coronado, 1987).

Limitations of genetic data derived from PCR

The theory that two distinct L-type Ca^{2+} channels are expressed in H9c2 cells originated from the electrophysiological results; the molecular genetic experiments were undertaken in order to confirm this interpretation and also to suggest an explicit structural basis for the results. Our approach was to use PCR to detect and amplify two distinct mRNA species from H9c2 cells. The polymerase chain reaction has the virtue of being very sensitive since it amplifies the number of copies of nucleic acid present in the original specimen many-fold (Gingeras *et al.* 1990). Using reverse transcriptase PCR, we have consistently detected two transcripts whose sequences exhibit high homology to the corresponding segments of the rabbit cardiac and skeletal muscle isoforms of the L-type Ca^{2+} channel. No PCR products were obtained when the reverse transcriptase was omitted from the initial reaction mixture, supporting the interpretation that we have amplified messenger RNA rather than contaminating genomic DNA. Unfortunately, this technique is non-quantitative; we can conclude that both transcripts were present, but we can say nothing about the relative intensity of their expression at the RNA level. In spite of the lack of such information, the electrophysiological recordings observed, e.g. the comparable slow and fast current densities in most cells and the ease with which both types of channels could be observed in single-channel recordings, hint that the two mature Ca^{2+} channel proteins are present in roughly equal numbers.

Ca^{2+} currents during myogenic differentiation

Although H9c2 cells originated from the embryonic rat ventricle, skeletal muscle properties can be induced after several passages (Kimes & Brandt, 1976). This observation gives reason to wonder whether the phenotypic changes that H9c2 cells apparently undergo during serial passages in culture could reflect de-differentiation to a developmental stage prior to the expression of muscle subtype-specific gene products. The simultaneous expression of cardiac and skeletal muscle isoforms of the L-type Ca^{2+} channel would exemplify such a phenomenon. This hypothesis would also be consistent with the fact that skeletal and cardiac muscle lineages diverge early during embryogenesis (Choi *et al.* 1989), after which committed cells express only the cardiac or the skeletal muscle L-type Ca^{2+} channel isoform (Rampe, Caffrey, Schneider & Brown, 1988; Caffrey, Brown & Schneider, 1989; DeHaan & Satin, 1990; Shih, Wathen, Marshall, Caffrey & Schneider, 1990). Although it is not known whether Ca^{2+} influx through L-type Ca^{2+} channels plays a significant role in myoblast differentiation, it has been suggested that the ontogeny of Ca^{2+} channels may involve intracellular events similar to those controlling the formation of other muscle-specific gene products (Shih *et al.* 1990). In any case, our results indicate that the H9c2 cell line may represent a useful experimental model with which to study aspects of cell commitment and development during myogenic differentiation. With such a model, the experimental manipulation of specific factors influencing cell differentiation may become possible.

REFERENCES

Adams, B. A. & Beam, K. G. (1989). A novel calcium current in dysgenic skeletal muscle. *Journal of General Physiology* **94**, 429–444.

Beam, K. G. & Knudson, M. (1988). Calcium currents in embryonic and neonatal mammalian skeletal muscle. *Journal of General Physiology* **91**, 781–798.

Bean, B. P. (1989). Classes of calcium channels in vertebrate cells. *Annual Review of Physiology* **51**, 367–384.

Caffrey, J. M., Brown, A. M. & Schneider, M. D. (1989). Ca^{2+} and Na^{+} currents in developing skeletal myoblasts are expressed in a sequential program: reversible suppression by transforming growth factor beta-1, an inhibitor of the myogenic pathway. *Journal of Neuroscience* **9**, 3443–3453.

Choi, J., Schultheiss, T., Lu, M., Wachtler, F., Kuruc, N., Franke, W. W., Bader, D., Fischman, D. A. & Holtzer, H. (1989). Founder cells for the cardiac and skeletal myogenic lineages. In *Cellular and Molecular Biology of Muscle Development*, ed. Kedes, L. H. & Stockdale, F. E., pp. 27–36. Alan R. Liss Co., New York.

COLQUHOUN, D. & SIGWORTH, F. J. (1983). Fitting and statistical analysis of single-channel records. In *Single-channel Recording*, ed. SAKMANN, B. & NEHER, E., pp. 191–263. Plenum Press, New York.

CORONADO, R. (1987). Planar bilayer reconstitution of calcium channels: lipid effects on single channel kinetics. *Circulation Research* **61**, suppl. 2, 46–52.

DEHAAN, R. L. & SATIN, J. (1990). The role of local cues in physiological differentiation of the embryonic heart: ion channel development. In *Molecular Biology of the Cardiovascular System*, ed. ROBERTS, R. & SCHNEIDER, M. D., pp. 73–98. Alan R. Liss Co., New York.

DONALDSON, P. L. & BEAM, K. G. (1983). Calcium currents in a fast-twitch skeletal muscle of the rat. *Journal of General Physiology* **82**, 449–468.

FELDMEYER, D., MELZER, W., POHL, B. & ZÖLLNER, P. (1992). Modulation of calcium current gating in frog skeletal muscle by conditioning depolarization. *Journal of Physiology* **457**, 639–653.

FOX, A. P., NOWYCKY, M. C. & TSIEN, R. W. (1987). Kinetic and pharmacological properties distinguishing three types of calcium currents in chick sensory neurones. *Journal of Physiology* **394**, 149–172.

GARCIA, J., AVILA-SAKAR, A. J. & STEFANI, E. (1990). Repetitive stimulation increases the activation rate of skeletal muscle calcium currents. *Pflügers Archiv* **416**, 210–212.

GINGERAS, T. R., DAVIS, G. R., WHITFIELD, K. M., CHAPPELLE, H. L., DIMICHELE, L. J. & KWOH, D. Y. (1990). A transcription-based amplification system. In *PCR Protocols: A Guide to Methods and Applications*, ed. INNIS, M., GELFAND, D., SNINSKY, J. & WHITE, T., pp. 245–252. Academic Press Inc., CA, USA.

GRAY, R. & JOHNSTON, D. (1987). Noradrenaline and β-adrenoceptor agonists increase activity of voltage-dependent calcium channels in hippocampal neurons. *Nature* **327**, 620–622.

HAMILL, O. P., MARTY, A., NEHER, E., SAKMANN, B. & SIGWORTH, F. J. (1981). Improved patch-clamp technique for high-resolution current recording from cells and cell-free membrane patches. *Pflügers Archiv* **391**, 85–100.

HAMILTON, S. L., MEJÍA-ALVAREZ, R., FILL, M., HAWKES, M. J., SCHILLING, W. P. & STEFANI, E. (1989). [^{3}H]PN200–110 and [^{3}H]ryanodine binding and reconstitution of ion channel activity with skeletal muscle membranes. *Analytical Biochemistry* **183**, 31–41.

HESCHELER, J., MEYER, R., PLANT, S., KRAUTWURST, D., ROSENTHAL, W. & SCHULTZ, G. (1991). Morphological, biochemical, and electrophysiological characterization of a clonal cell (H9c2) line from rat heart. *Circulation Research* **69**, 1476–1486.

HESS, P., LANSMAN, J. B. & TSIEN, R. W. (1984). Different modes of Ca^{2+} channel gating behavior favored by dihydropyridine Ca^{2+} agonists and antagonists. *Nature* **311**, 538–544.

HESS, P. & TSIEN, R. W. (1984). Mechanism of ion permeation through calcium channels. *Nature* **309**, 453–456.

HIRANO, Y., FOZZARD, H. A. & JANUARY, C. T. (1989). Characteristics of L-type and T-type Ca^{2+} currents in canine cardiac Purkinje cells. *American Journal of Physiology* **256**, H1478–1492.

ISENBERG, G. & KLÖCKNER, U. (1982). Calcium currents of isolated bovine ventricular myocytes are fast and of large amplitude. *Pflügers Archiv* **395**, 30–41.

KIMES, B. W. & BRANDT, B. L. (1976). Properties of a clonal muscle cell line from rat heart. *Experimental Cell Research* **98**, 367–381.

LACERDA, A. E. & BROWN, A. M. (1989). Nonmodal gating of cardiac calcium channels as revealed by dihydropyridines. *Journal of General Physiology* **93**, 1243–1273.

LEE, K. S. & TSIEN, R. W. (1984). High selectivity of calcium channels in single dialysed heart cells of the guinea-pig. *Journal of Physiology* **354**, 253–272.

MA, J. & CORONADO, R. (1988). Heterogeneity of conductance states in calcium channels of skeletal muscle. *Biophysical Journal* **53**, 387–395.

MA, J., MUNDIÑA-WEILENMANN, C., HOSEY, M. M. & RÍOS, E. (1991). Dihydropyridine-sensitive skeletal muscle Ca channels in polarized planar bilayers. *Biophysical Journal* **60**, 890–901.

MCLAUGHLIN, S. G. A., SZABO, G. & EISENMAN, G. (1971). Divalent ions and the surface potential of charged phospholipid membranes. *Journal of General Physiology* **58**, 667–687.

MEJÍA-ALVAREZ, R., FILL, M. & STEFANI, E. (1991). Voltage-dependent inactivation of T-tubular skeletal calcium channels in planar lipid bilayers. *Journal of General Physiology* **93**, 393–412.

MEJÍA-ALVAREZ, R., SIPIDO, K. R. & MARBAN, E. (1992). Expression of two isoforms of the L-type calcium channel in single cells from a clonal muscle cell line. *Biophysical Journal* **61**, 408A.

MIKAMI, A., IMOTO, K., TANABE, T., NIIDOME, T., MORI, Y., TAKESHIMA, H., NARUMIYA, S. & NUMA, S. (1989). Primary structure and functional expression of the cardiac dihydropyridine-sensitive calcium channel. *Nature* **340**, 230–233.

RAMPE, D. E., CAFFREY, J. M., SCHNEIDER, M. D. & BROWN, A. M. (1988). Control of the expression of the 1,4-dihydropyridine receptor in BC3H1 cells. *Biochemical and Biophysical Research Communications* **152**, 769–775.

ROSENBERG, R. L., HESS, P., REEVES, J. P., SMILOWITZ, H. & TSIEN, R. (1986). Calcium channels in planar lipid bilayers: Insights into mechanisms of ion permeation and gating. *Science* **231**, 1564–1566.

SANCHEZ, J. A. & STEFANI, E. (1983). Kinetic properties of calcium channels of twitch muscle fibres of the frog. *Journal of Physiology* **337**, 1–17.

SHIH, H. T., WATHEN, M. S., MARSHALL, H. B., CAFFREY, J. M. & SCHNEIDER, M. D. (1990). Dihydropyridine receptor gene expression is regulated by inhibitors of myogenesis and is relatively insensitive to denervation. *Journal of Clinical Investigation* **85**, 781–789.

SIPIDO, K. R. & MARBAN, E. (1991). L-type calcium channels, potassium channels, and novel nonspecific cation channels in a clonal muscle cell line derived from embryonic rat ventricle. *Circulation Research* **69**, 1487–1499.

TANABE, T., TAKESHIMA, K., MIKAMI, A., FLOCKERZI, V., TAKAHASHI, H., KANGAWA, K., KOJIMA, M., MATSUO, H., HIROSE, T. & NUMA, S. (1987). Primary structure of the receptor for calcium channel blockers from skeletal muscle. *Nature* **328**, 313–318.

TOMASELLI, G. F., FELDMAN, A. M., YELLEN, G. & MARBAN, E. (1990). Human cardiac sodium channels expressed in *Xenopus* oocytes. *American Journal of Physiology* **258**, H903–906.

TRAUTWEIN, W. & PELZER, D. (1985). Gating of single calcium channels in the membrane of enzymatically isolated ventricular myocytes from adult mammalian hearts. In *Cardiac Electrophysiology and Arrhythmias*, ed. ZIPES, D. P. & JALIFE, J., pp. 31–42. Grune and Stratton, Orlando, FL, USA.

WILLIAMS, M. E., FELDMAN, D. H., MCCUE, A. F., BRENNER, R., VELICELEBI, G., ELLIS, S. B. & HARPOLD, M. M. (1992). Structure and functional expression of α_1, α_2, and β subunits of a novel human neuronal calcium channel subtype. *Neuron* **8**, 71–84.

YUE, D. T. & MARBAN, E. (1990). Permeation in the dihydropyridine-sensitive calcium channel. Multi-ion occupancy but no anomalous mole-fraction effect between Ba^{2+} and Ca^{2+}. *Journal of General Physiology* **95**, 911–939.

Acknowledgements
We would like to thank Kimberley Kluge for valuable technical assistance in the cell culture and molecular biology experiments. This investigation was supported by grants to E. M. (National Institutes of Health (NIH) RO1 HL36957), and to G. F. T. (NIH Clinician Investigator Award K08 HL 02421).

Author's present address
R. Mejía-Alvarez: Departamento de Fisiología, Instituto Nacional de Cardiología, Juan Badiano no. 1, México DF 14080, México.

Received 17 March 1993; accepted 23 November 1993.